



Politecnico di Bari

Repository Istituzionale dei Prodotti della Ricerca del Politecnico di Bari

Looking at NB-IoT over LEO Satellite Systems: Design and Evaluation of a Service-Oriented Solution

This is a post print of the following article

Original Citation:

Looking at NB-IoT over LEO Satellite Systems: Design and Evaluation of a Service-Oriented Solution / Sciddurlo, Giancarlo; Petrosino, Antonio; Quadrini, Mattia; Roseti, Cesare; Striccoli, Domenico; Zampognaro, Francesco; Luglio, Michele; Perticaroli, Stefano; Mosca, Antonio; Lombardi, Francesco; Micheli, Ivan; Ornatelli, Antonio; Schena, Vincenzo; Di Mezza, Alessandro; Mattioni, Alessio; Morbidelli, Daniele; Boggia, Gennaro; Piro, Giuseppe. - In: IEEE INTERNET OF THINGS JOURNAL. - ISSN 2327-4662. - ELETTRONICO. - 9:16(2022), pp. 14952-14964.

[10.1109/JIOT.2021.3135060]

Availability:

This version is available at <http://hdl.handle.net/11589/231966> since: 2024-01-03

Published version

DOI:10.1109/JIOT.2021.3135060

Publisher:

Terms of use:

(Article begins on next page)

Looking at NB-IoT over LEO Satellite Systems: Design and Evaluation of a Service-Oriented Solution

G. Sciddurlo, A. Petrosino, M. Quadrini, C. Roseti, D. Striccoli, F. Zampognaro, M. Luglio, S. Perticaroli, A. Mosca, F. Lombardi, I. Micheli, A. Ornatelli, V. Schena, A. Di Mezza, A. Mattioni, D. Morbidelli, G. Boggia, and G. Piro

The adoption of the NB-IoT technology in satellite communications intends to boost Internet of Things services beyond the boundaries imposed by the current terrestrial infrastructures. Apart from link-level studies in the scientific literature and preliminary 3GPP technical reports, the overall debate is still open. To provide a further step forward in this direction, the work presented herein pursues a novel service-oriented methodology to design an effective solution, meticulously stitched around application requirements and technological constraints. To this end, it conducts link-level and system-level investigations to tune physical transmissions, satellite constellation, and protocol architecture, while ensuring the expected system behavior. To offer a real smart agriculture service operating in Europe, the resulting solution exploits 24 Low Earth Orbit satellites, grouped into 8 different orbits, moving at an altitude of 500 km. The configured protocol stack supports the transmission of tens of bytes generated at the application layer, by also counteracting the issues introduced by the satellite link. Since each satellite has the whole protocol stack on-board, terminals can transmit data without the need for the feeder link. This ensures communication latencies ranging from 16 minutes to 75 minutes, depending on the served number of terminals and the physical transmission settings. Moreover, the usage of the Early Data Transmission scheme reduces communication latencies up to 40%. These results pave the way towards the deployment of an effective proof-of-concept, which drastically reduces the time-to-market imposed by the current state of the art.

Index Terms—NB-IoT, satellite communication, system design, link-level analysis, system-level evaluation.

I. INTRODUCTION

Narrowband-Internet of Things (NB-IoT) has been standardized by the 3GPP in Release-13 for serving Internet of Things (IoT) devices through the mobile network infrastructure [1]. The widespread growth of IoT applications is currently embracing some challenging scenarios, including those concerning devices deployed in geographical areas where

terrestrial networks are not present or hard to reach (for instance deserts, oceans, or forests). Here, service continuity and fast service deployment can be successfully achieved only by leveraging disruptive methodologies that go beyond the boundaries imposed by current terrestrial networks.

Recently, the scientific literature and the 3GPP standardization body considered as viable the integration of NB-IoT in satellite-based architectures. Without any doubt, the design of the space segment is not easy. A number of state of the art contributions already tackled the related operational technical challenges, while focusing on feasibility studies at both physical and link levels [2]–[11], satellite constellation [5], [9], and Random Access procedure [3], [10], [11]. However, aside from the important findings they report, detailed selection of physical (and standards-compliant) transmission settings, protocol stack configuration, and a significant system-level evaluation of the overall communication architecture are still unexplored topics. Also, the discussion started by the 3GPP in RAN2 technical meetings (see [12] and [13]) is still in its embryonic stage and no turnkey solutions have been standardized yet.

To bridge this gap, the work presented herein addresses the design of a fully functional NB-IoT over satellite service, compliant with 3GPP specifications, and aiming to face the most critical issues arising from the employment of NB-IoT over Non-Terrestrial Networks (NTNs) into a real application scenario¹.

Differently from the current scientific literature, it follows a service-oriented methodology that:

- illustrates application requirements and technological constraints that characterize a reference use case (taken from the smart agriculture domain);
- configures the whole protocol stack for ensuring the transmission of tens of bytes generated at the application layer within a single data packet, even in the absence of a feeder link;
- identifies low-level adaptations for counteracting the issues that affect the satellite communication during the random access procedure, Doppler shift, and frequency carrier offset;

G. Sciddurlo, A. Petrosino, D. Striccoli, G. Piro, and G. Boggia are with the Department of Electrical and Information Engineering (DEI), Politecnico di Bari, Italy, and with Consorzio Nazionale Interuniversitario per le Telecomunicazioni (CNIT). M. Luglio, M. Quadrini, C. Roseti, and F. Zampognaro are with University of Rome “Tor Vergata”. S. Perticaroli, A. Mosca, F. Lombardi are with Radio Analog Micro Electronics (RAME) srl. I. Micheli, A. Ornatelli, and V. Schena are with Thales Alenia Space Italia (TASI). A. Di Mezza, A. Mattioni, and D. Morbidelli are with RINA Consulting SpA.

This work was funded by the European Space Agency, contract no.4000129810/20/NL/CLP. The authors would like to thank Dr. Stefano Cioni, Dr. Nicolò Mazzali and Frank Zeppenfeldt (all with ESA) for the precious help. Opinions, interpretations, recommendations, and conclusions presented in this paper are those of the authors and are not necessarily endorsed by ESA.

¹This paper is the result of research activities carried out by different academic and industrial partners, collaborating as a partnership in the context of the project “3GPP Narrow-Band Internet-of-Things (NB-IoT) User Sensor Integration into Satellite” funded by the European Space Agency (ESA) under contract no. 4000129810/20/NL/CLP, <https://artes.esa.int/projects/nbiot4space>

- conducts an accurate link-level investigation to retrieve physical settings that guarantee an effective ground-satellite communication;
- defines a satellite constellation offering a realistic service operating in Europe;
- investigates the performance of the conceived architecture through system-level simulations.

Obtained results demonstrate that a constellation of 24 Low Earth Orbit (LEO) satellites, grouped into 8 different orbits and moving at an altitude of 500 km ensures communication latencies ranging from 16 minutes to 75 minutes, depending on the served number of terminals and the physical transmission settings. At the same time, the adoption of the Early Data Transmission scheme can reduce communication latencies up to 40%. By reducing the number of satellites per orbit (from 3 to 2), it is still possible to drain all the generated data, but at the cost of a much higher average communication latency.

The remainder of this paper is organized as reported below. Section II introduces the NB-IoT technology and presents the state of the art addressing the integration of NB-IoT in satellite architectures. Section III describes the reference scenario taken into account in this contribution and clarifies the targeted system requirements. Section IV illustrates the overall protocol architecture and reviews the low-level adaptations to be integrated. Section V provides a link-level study and develops the satellite constellation. Starting from these outcomes, Section VI investigates, through system-level simulations, the overall performance of the proposed NTN-based communication system. Finally, Section VII provides the conclusions of this paper and draws future research activities and developments.

II. STATE OF THE ART ON NB-IoT OVER SATELLITE SYSTEMS

The review of the state of the art is organized as in what follows: first, the NB-IoT technology, standardized by 3GPP in Release-13 is presented in Section II-A; scientific contributions focusing on NB-IoT over satellite systems are discussed in Section II-B; finally, recent 3GPP activities on NTN networks are illustrated in Section II-C. These two latter Sections also note the scientific and technical lacks covered by this work.

A. The NB-IoT technology

NB-IoT is a powerful communication technology for Low Power Wide Area Network (LPWAN). Standardized by 3GPP in Release-13, it implements terrestrial communications for a high number of devices, over large areas, at a low cost, and with a long battery life [14].

NB-IoT uses a subset of the well-known Long Term Evolution (LTE) technological features while limiting its operation to a single carrier bandwidth of 180 kHz (narrow-band technology) [15]. Similarly to LTE, the downlink is based on the Orthogonal Frequency Division Multiplexing (OFDM) transmission scheme, with 12 subcarriers and 15 kHz subcarrier spacing [16]. The frame lasts 10 ms and consists of 10 subframes of 1 ms each. In turn, the single subframe embraces two slots with seven OFDM symbols. The uplink is based

on the Single Carrier Frequency Division Multiple Access (SC-FDMA) transmission scheme. It differs from LTE. Two possible configurations, namely single-tone and multi-tone, are supported. The multi-tone configuration still uses a subcarrier spacing of 15 kHz. The Resource Unit, which represents the smallest radio resource that can be allocated to the end-user [17], spans over 3, 6, or 12 adjacent subcarriers and lasts 4 ms, 2 ms, or 1 ms, respectively [18]. The single-tone configuration, instead, can operate with a subcarrier spacing equal to 15 kHz or 3.75 kHz. However, in this case, only one subcarrier can be used by a single user. Depending on the subcarrier spacing, the uplink bandwidth is divided into 12 or 48 Resource Units lasting 8 ms and 32 ms, respectively [18].

B. Related Works on NB-IoT over satellite links

The scientific literature investigated the possibility to use NB-IoT (with specific adaptations) in satellite-based communication systems. As summarized in Table I, available studies focus the attention on the analysis and the selection of a suitable antenna type [2]–[4], the evaluation of the link budget [2]–[8], the design of a satellite constellation [5], [9], the study of link-level performance [2], [8], the evaluation of the Doppler shift [3], [4], [6], [8]–[11], and the management of the Random Access procedure [3], [10], [11]. Other interesting related works, such as [19] and [20], investigate Doppler shift and Random Access procedure in satellite communication systems based on LTE and 5G, respectively. Focusing the attention on specific aspects of the system and in the absence of uniform assumptions, these studies appear isolated. Nevertheless, the effective deployment of NB-IoT over satellite links requires a service-oriented approach where protocols, architectural, physical, and functional aspects are accounted for altogether. In this sense, the main contribution of this paper is to describe every aspect of interest, by reviewing, enhancing, redefining, modelling, and simulating it in the context of an exhaustive proof of the feasibility of the target solution, while endorsing the compelling capabilities allowed by regenerative satellites.

C. Recent 3GPP discussions

The 3GPP started the standardization of NTN in Release-15, addressing deployment scenarios, related system parameters (e.g., architecture, satellite altitude, orbit), and adapted channel models [21]. Available reports and specifications use the concept of narrow-band access (already introduced with NB-IoT) to characterize a service-link provided by a mobile satellite in the frequency band below 6 GHz. Moreover, they define two possible deployment scenarios. The *wide area IoT service* intends to provide a global continuity of service to a group of moving sensors in areas partially covered by terrestrial networks. The *local area IoT service*, instead, is conceived for a group of sensors able to collect data and report to a central point installed on a moving platform. In this case, the satellite has to guarantee the connectivity between the mobile core network and the base stations serving IoT devices. In both cases, 3GPP remarks the optional integration of the Inter Satellite Link (ISL) and the possibility to consider either a

TABLE I
REVIEW OF RELATED WORKS

Features	[2]	[3]	[4]	[5]	[6]	[7]	[8]	[9]	[10]	[11]	[19]	[20]	This work
NB-IoT in satellite communications	✓	✓	✓	✓	✓	✓	✓	✓	✓	✓			✓
Antenna Selection	✓	✓	✓										✓
Link Budget Evaluation	✓	✓	✓	✓	✓	✓	✓						✓
Constellation Design				✓				✓					✓
Visibility Time													✓
BLER curves Analysis	✓						✓						✓
Doppler shift Evaluation		✓	✓		✓		✓	✓	✓	✓	✓	✓	✓
Random Access procedure		✓							✓	✓	✓	✓	✓
Protocol Stack Configuration													✓
System-level Architectural Design													✓
System-level Performance Analysis													✓

satellite with bent-pipe payload or the implementation of the base station on-board the satellite.

More recently, with Release-17, 3GPP proposed new amendments from Physical (PHY) to Non-Access Stratum (NAS) layers, aiming to improve performances of NTN in terms of latency, coverage, and power consumption [22]. Particularly interesting is the discussion presented in [13], whose goal is to investigate the applicability of [12] in NTN deployments for explicit support of IoT services based on NB-IoT.

As anticipated in Section I, 3GPP activities on NTN networks are not complete. Therefore, this paper leverages all the guidelines proposed by preliminary 3GPP technical reports and pursues the ambitious goal to provide concrete answers to the open questions recently arisen from 3GPP.

III. THE REFERENCE USE CASE AND RELATED REQUIREMENTS

The reference use case taken into account in this work refers to the smart agriculture scenario, which represents one of the most promising application fields, where NB-IoT technology over satellite can be effectively employed.

As well-known, farms require constant and continuous connection and communication with monitoring systems employed for different purposes (i.e., harvest management, power consumption of machines and facilities, optimization of production processes, or environmental control for greenhouse and open field management) [23]–[25]. In this context, satellites play a key role to answer the challenges of future farming, especially for large customers that require hundreds or thousands of NB-IoT devices for precision farming in rural areas. This is testified by several companies that are leveraging LEO satellite-based connections to deliver seamless, real-time communications in 100% of the globe [26]. Currently, there are also initiatives aiming to help mobile operators to accelerate the process of deploying new NB-IoT devices and services connected through satellite-based systems in smart agriculture scenarios [27].

These motivations are also based on the project funded by the European Space Agency (ESA), mentioned in Section I, which considers the smart agriculture scenario as one of the most interesting case studies.

Without loss of generality, this study assumes that clusters of IoT devices are distributed in the geographical area covered

by the satellite. Each cluster is deployed in a rectangular crop field of size 30 hectares. This is about the maximum size of a crop field as present in some European countries [25]. A so large field size allows evaluating the system performance for a wide area covered by a high number of sensors. Sensor nodes are supposed to be placed uniformly in the whole field, with a 10 m inter-spacing. Therefore, a total number of 3000 nodes can be deployed in each cluster.

Like in the vast majority of smart agriculture scenarios, wireless sensor units deployed on-ground are characterized by four different types of components, i.e., the application-specific sensors, the processing unit, the radio transceiver, and the battery power [23]. The energy needed by each sensor is almost totally consumed by the radio transceiver when the node is active, so it depends on the time interval needed by the node to successfully transmit its generated measurement. Nevertheless, the node is active only during the Random Access procedures and the TB transmissions, each one taking not more than tens of milliseconds. Since a sensor node is active for a small fraction of time a day, monitoring sensors operated in smart agriculture can effectively exploit embedded rechargeable batteries powered by solar cells that are enough for the system to work properly, as testified by several works found in the literature [23], [28]–[32]. As a consequence, energy consumption is not a relevant issue in the considered application scenario, and its impact on the system performance can be neglected in this study.

In the use case under analysis, portable sensors are used to measure five different soil-related parameters for monitoring purposes: soil moisture, rain/water flow, soil temperature, conductivity, and salinity [23]. These sensed measurements are collected with a 2-byte precision each. In addition, 2 bytes of sensor ID (65536 different sensors can be addressed, which is enough for the depicted scenario) are included to identify the specific sensor data come from. Finally, 6 additional bytes of latitude/longitude coordinates from a GPS module are added to the generated message, to locate the position of the sensed data with high accuracy. The whole size of the message generated by each sensor is thus 18 bytes at the application layer.

To monitor the field efficiently, the sensed parameters do not need to be generated with a high frequency. So, it is supposed that all the five measurements are collected by each node 6 times per day, i.e., a measurement of each type is collected every 4 hours by each sensor node. Furthermore, this very

low frequency of data generation can be easily manageable by the network since it allows each node to exploit the visibility time of more satellites (passing over the field) to transmit its own data. To this end, sensed data are collected by the node and buffered until the node enters the satellite visibility time. During this time interval, the node attempts to send the content of the buffer to the base station on the satellite until its successful reception.

Regarding the system requirements, this work intends to fulfil the following challenging aspects:

- **NB-IoT compliance:** the adoption of standard 3GPP technology shall be endorsed as much as possible with the aim to support device interoperability, application extendability, and cost-efficiency. In particular, it is necessary to provide a solution with simplified hardware, which guarantees a long battery life.
- **Guarantee of a service area and timing compliant with application characteristics:** satellite coverage shall be ensured in the service area with an interval of a few hours, allowing the sensors to transmit data within this interval.
- **Need for a proper satellite configuration to cover the entire zone of interest:** the satellite system is designed to cover the European zone of interest, which is a portion of about 6700 km of the Earth surface of 60° longitude, starting from 20° west to 40° east.
- **Data transfer accomplishment within the visibility time:** the visibility time represents the period during which the NTN terminal can set up a radio bearer and perform the data transmission towards the satellite. A transmission round shall be shorter than the visibility time, which in turn is a function of the satellite orbit characteristics and the achieved link budget.
- **Satellite access latency shall not significantly shrink the time window for sensor data transmission:** the average amount of time required for finalizing the Random Access procedures is the first delay contribution that is inflated by the satellite Round Trip Delay (RTD). Such a setup delay shall be at least an order of magnitude lower than the overall visibility time, in order to not impair actual data transmission.
- **The satellite link shall support the reliable communication:** satellite provides a wireless channel significantly affected by several propagation impairments. Specifically, propagation losses on the ground-space link are due to different contributions, including absorption of the atmosphere, attenuation by rain, scintillation of troposphere and ionosphere, depolarization effects, and fog and atmospheric gas attenuation. All of these essential aspects should be taken into account to identify suitable physical layer settings and system configurations that guarantee reliable communication.
- **Doppler effect compensation:** because of the movement of the satellite, a shift in the frequency domain will occur. The Doppler shift requires adaptations at the physical layer.
- **Need for a communication infrastructure resilient to**

feeder-link unavailability: the connection between the satellite and the rest of the NB-IoT network functional elements is not guaranteed over time. The feeder-link is set up when a gateway is under the satellite spot-beam and this might be time-shifted with respect to service-link availability. As a consequence, the whole architecture shall be designed in order to allow NTN terminals to exchange data with satellites, even in the temporary absence of the feeder-link.

- **Optimization of the satellite cost:** the decoupling of the satellite service and feeder-link poses the problem of how to guarantee an end-to-end service. Solutions can embrace the setup of a satellite constellation and the deployment of on-board processing.

IV. PROTOCOL ARCHITECTURE AND LOW-LEVEL ADAPTATIONS

In line with 3GPP standardization activities on NTN networks [21], the architecture considered in this work implements the *Local Area IoT Service* scenario.

As for the baseline satellite infrastructure, the reference architecture embraces NTN terminals, satellite, and NTN-Gateway. NTN terminals and satellite exchange data through the *service-link*. In particular, the NTN terminal can establish a connection with a single satellite of the constellation during its visibility period. Indeed, when a new satellite belonging to the same orbit passes over the area where the aforementioned NTN terminal is deployed, that device restarts the configuration procedures in a stateless way. On the other hand, satellite and NTN-Gateway interact with each other through the *feeder-link*. The NTN-Gateway could be located in a different geographical area, thus leading to a time-shifted contact over a feeder-link with the serving satellite.

In this paper, the network architecture design is driven by the requirement of decoupling service-link and feeder-link. Therefore, since the feeder-link availability is not always guaranteed, data transmissions through the service-link can be still implemented asynchronously with respect to the data offload to the NTN-Gateway. To this end, the conceived solution assumes to install the full Evolved Packet System (EPS) protocol stack on-board the satellite. The overall service can be implemented through a satellite constellation without ISL. Indeed, possible configurations that exploit ISL and multiple gateways are not considered and the resulting solution ensures a significant reduction of both complexity and costs. Such an important technical choice has been initially considered by the Cellular IoT (CIoT) architecture [33]. But, at the time of this writing and to the best of the authors' knowledge, it has never been investigated from the system-level perspective, representing an attractive solution for international companies, like ESA, working on satellite systems.

Fig. 1 depicts the proposed network architecture and the resulting protocol stack. The satellite hosts different logical nodes, including evolved NodeB (eNB), CIoT-Serving Gateway Node (C-SGN), and Local Break-Out (LBO). The eNB, that is the base station, implements the Uu interface offering the radio connectivity with NTN terminals. C-SGN

implements the functionalities of the rest of the EPC protocol stack. For this reason, it includes:

- the Mobility Management Entity (MME) handles Control Plane communications by means of NAS signalling supported by Radio Resource Control (RRC) protocol;
- the Serving Gateway (S-GW) and the Packet Gateway (P-GW) handle User Plane communications supported by IP at a higher layer;
- the Home Subscriber Server (HSS) is in charge of the NTN terminal network registration and authentication.

To support the asynchronous data delivery, messages delivered by NTN terminals through service-link are temporarily stored on-board the satellite, by leveraging a local application implemented through the LBO. Collected data can be offloaded to a remote NTN-Gateway (on the ground) as soon as it will be in the line of sight with the satellite. To embrace multiple possibilities at the same time, the feeder-link can be implemented by using non-3GPP technologies, offering data rates comparable or higher than those registered in the uplink direction.

Starting from the afore described high-level protocol architecture, some specific adaptations must be integrated into different levels of the communication stack for properly counteracting the issues introduced by the satellite communication link.

A. Selected adaptations for the Uu interface

Regarding the Uu interface, adaptations are required for both Control Plane and User Plane [34]. A new method for uplink transmission, called Non-IP Data Delivery (NIDD), is available and allows to encapsulate user data in NAS messages of the Control Plane, involving both MME and Service Capabilities Exposure Function (SCEF) components, as an alternative to IP-based data transport. NIDD introduces an overhead of 6 bytes due to the header size of the NAS message. Furthermore, new RRC procedures available since Release-15 allow suspending and (then) quickly resume the RRC connection, which is very useful considering the limited visibility intervals.

As specified in Section III, the total size of each message coming from a sensor node is equal to 18 bytes. At the application layer, the Constrained Application Protocol (CoAP) protocol is chosen [35], introducing an associated 4 bytes of overhead. It is a web-based protocol that relies upon the request-response (or client-server) paradigm and asynchronous data exchange. These two features are both suitable for the considered scenario, where sensors exchange data on-demand and with a low frequency. NIDD is selected at the transport layer as an alternative to the canonical UDP/IP solution. In fact, CoAP is compatible with NIDD, leading to an overhead reduction from 28 bytes of the UDP/IP solution to 6 bytes, as described above.

At lower layers, Packet Data Convergence Protocol (PDCP), Radio Link Control (RLC) and Medium Access Control (MAC) protocols have been properly configured to meet NTN NB-IoT constraints and associated requirements. To this end, data retransmissions have been demanded to the MAC layer

only, i.e., enabling the Hybrid Automatic Repeat Request (HARQ) process, disabling retransmission and feedback-based procedures at PDCP and RLC layers. Furthermore, Protocol Data Unit (PDU) segmentation at the RLC layer has been disabled. This in turn translates into the possibility to use PDUs with an extremely simplified header for all the three layers [36]–[38], adding a minimum of 4 bytes of overhead.

In conclusion, with the proposed configuration, account is taken for 18 bytes for data, 4 bytes for application, 6 bytes for NIDD and a total of 4 bytes for all lower layers (i.e., PDCP, RLC and MAC). Consequently, the smallest transport block that fits one of the possible options for the Transport Block Size (TBS), enabling the opportunity to exploit the Early Data Transmission (EDT) protocol in the proposed solution, is equal to 41 bytes (328 bits), as specified in [39].

B. Selected adaptations for the Random Access procedure

The Random Access procedure is exploited by NTN terminals to acquire the uplink resources needed for data transmission.

First of all, the network needs to know which Random Access Occasion (RAO) a preamble belongs to, in order to determine the correct Timing Advance (TA) for the synchronization of the uplink transmission.

If the periodicity of the RAO is not large enough, the preamble receiving windows of two consecutive RAOs could overlap each other, creating ambiguity on the RAO a preamble belongs to. An excellent solution to avoid this issue, investigated in [12], is to extend the interval between two RAOs to an amount greater than two times the maximum delay difference experienced by two NTN terminals within the same cell.

Enhancements to the Timing Advance are required as well. The TA command exceeds the maximum value allowed by the standard, which covers a distance of at most 100 km between the NTN terminal and the satellite [11]. To cope with this issue, the most promising solutions consider an autonomous TA calculation by the NTN terminal. It exploits the Global Navigation Satellite System (GNSS) to derive its position and the satellite ephemeris provided by the network to estimate the propagation delay through geometric formulas [40]. An alternative solution to GNSS is to broadcast a common TA offset related to a reference point located at the center of the beam (Nadir). The differential part of the TA, evaluated for the NTN terminal with respect to the reference point, can be compensated by the TA command without introducing any modification to the standard since it falls in the 100 km range also in the worst case of an NTN terminal at the cell edge.

Even if the majority of these solutions must be better investigated through experimental testbeds, these adaptations have been selected as the most appropriate choices for the scenario under analysis.

C. Selected adaptations for Doppler Shift and Carrier Frequency Offset

In satellite communication, two undesirable effects emerge in the frequency domain: the Doppler shift and the Carrier Frequency Offset (CFO). The former is caused by the relative

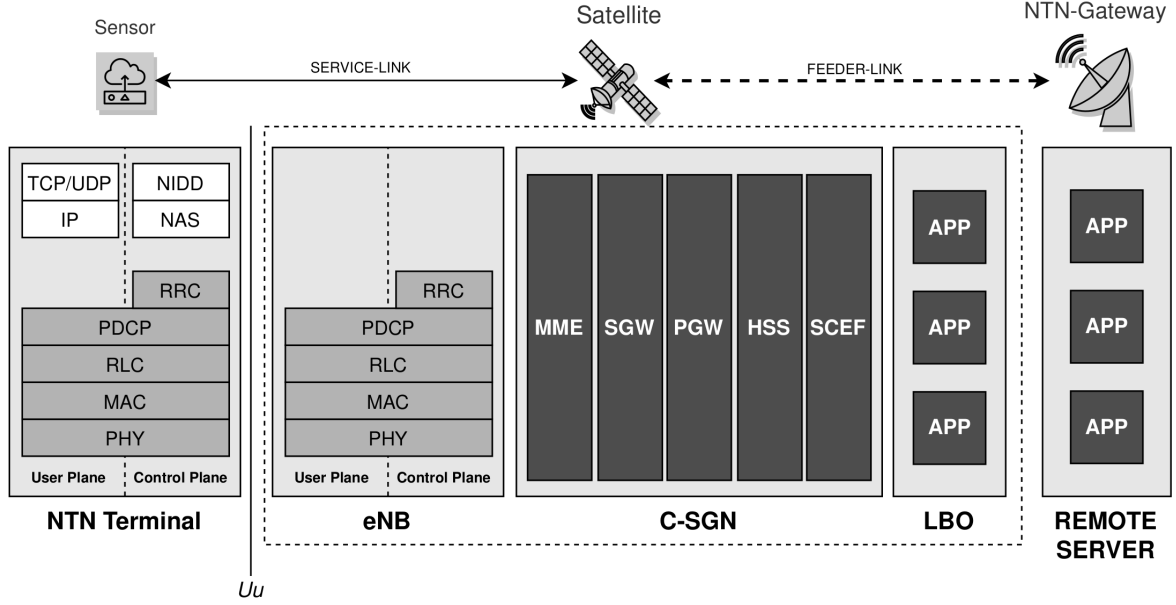


Fig. 1. The proposed network architecture and the protocol stack of the NTN terminal and satellite.

movement between the NTN terminal and the satellite. Since in the selected scenario the NTN terminals are fixed on the ground, it is exclusively due to the satellite movement. The latter, instead, describes the frequency shift given by the inaccuracy of the receiver local oscillators. These two effects produce a frequency shift that causes interference in adjacent subcarriers in the uplink, thus posing a relevant issue for signal reception.

According to [20], a maximum Doppler shift of 950 Hz can be tolerated by the LTE physical layer. Nevertheless, by following the model presented in [19] and the indications provided in [12], the scenario considered in this work will experience a Doppler shift from -30 kHz to 30 kHz. Because these values are much more above the tolerated limit of 950 Hz, additional methodologies must be integrated into the adapted Uu interface to achieve Doppler compensation. Also for the CFO, it is necessary to introduce compensation techniques. Following 3GPP specifications, in fact, where an NTN terminal crystal accuracy can be 10 ppm, a CFO of about 20 kHz is derived at the carrier frequency chosen in the reference scenario [12].

The Uu interface conceived in this work may integrate two suitable solutions for the Doppler shift compensation. The first is based on the standard recommendations and makes use of GNSS capable devices with the knowledge of the satellite ephemeris so that the position of the satellite and the relative distance from it can be estimated autonomously by NTN terminals.

The second solution refers to not GNSS-enabled devices. It starts from the study carried out in [9], which aims to jointly compensate the Doppler shift and the CFO. If compared to the Doppler shift, the CFO has a constant value during the whole satellite visibility. Given the absence of any positioning information, an estimator can be used, based on the prior knowledge of the expected Doppler Shift, which is always

contained within the maximum deviation range computed for the selected scenario. To perform a correct initial Doppler shift estimation and compensation, the filter bandwidth is widened by a frequency range that includes the maximum Doppler shift and the CFO, so that it can always contain the modulated signal affected by the total frequency shift. Then the Doppler shift estimation is updated periodically through a first-order differential system. It is able to track and compensate the Doppler variations in time, with a periodicity that allows the inclusion of shift variation into the 950 Hz value. Accordingly, an 80 ms periodicity is sufficient to satisfy the Doppler compensation rate during all the satellite visibility periods.

V. LINK-LEVEL ANALYSIS AND SATELLITE CONSTELLATION

The design of an effective communication architecture that leverages the NB-IoT technology over a satellite-link grounds its roots on a deep investigation of link-level features.

A. Antenna Selection

Regarding the NTN terminal, the antenna must be easily deployable, at a low cost. For this reason, the solution considered in this work adopts a monopole antenna with linear polarization, installed horizontally-oriented. Such an antenna type is already available as a Commercial-Off-The-Shelf (COTS) product [41].

Regarding the satellite, it is important to keep the best trade-off between the amount of power radiated by the antenna and the High Power Amplifier (HPA), which is responsible to generate such power. Small satellites cannot host a large HPA. But, to counteract the reduced power resource offered by a small HPA, it is possible to increase the radiated power

by working on the antenna gain. However, it is not possible to overstate in this direction because a high antenna gain translates to an increased volume, mass, and deployment complexity. Based on these aspects, this work considers a tile circular patch antenna for the satellite, whose deployment must be managed by taking into account the possible dynamical steady states of the satellite orbit. Moreover, the signal generated by a monopole antenna, with linear polarization, experiences a polarization rotation when propagating through the Earth's ionosphere (because of the impact of the Earth's magnetic field). Consequently, the satellite may receive a signal with a polarization different from the one expected by its receiving antenna. This generally worsens communication performance. An antenna with circular polarization at the satellite side, however, partially mitigates this effect. In this context, the worst case of misalignment between circular and linear polarization, equal to 45° , produces a penalty of 3 dB. Note that the tile circular patch antenna offers good performance regarding the coverage of the satellite beam. The Half Power Beam Width (HPBW) factor represents the angle in which the relative power is higher than the 50% of the peak power of the main lobe reported in the effective radiated field of the antenna. The main lobe of the selected antenna ensures $\pm 56^\circ$ HPBW, thus resulting in a very suitable choice for the scenario under study.

In both cases, the selected antennas offer a not negligible gain, equal to 5.19 dB for the one installed on the NTN terminal and 6.97 dB for the antenna patch hosted by the satellite. Please note that these values have been calculated by considering the analytical formulation presented in [41] and by leveraging (for the satellite only) a linear approximation in the frequency range spanning from 1900 MHz to 2200 MHz.

To conclude, Fig. 2 shows additional details on the selected antenna types, also reporting the related radiation diagrams.

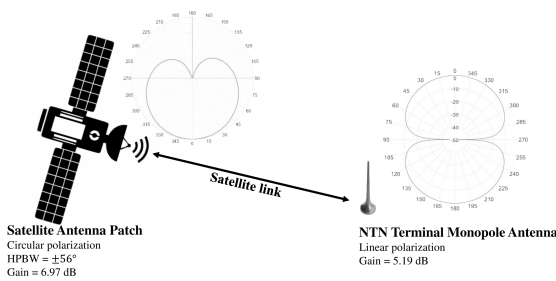


Fig. 2. Proposed antennas types and related radiation diagrams.

B. Link Budget Analysis

Given the power gain offered by the selected antennas, the transmission power imposed by the NB-IoT technology, and the propagation losses, the link budget analysis allows obtaining the satellite antenna altitude and the range of elevation angles at which the radio link could be established. The link budget evaluation is based on the analysis carried out in [42] for satellite communications systems. The design of the satellite system is based on theoretical formulas that accurately

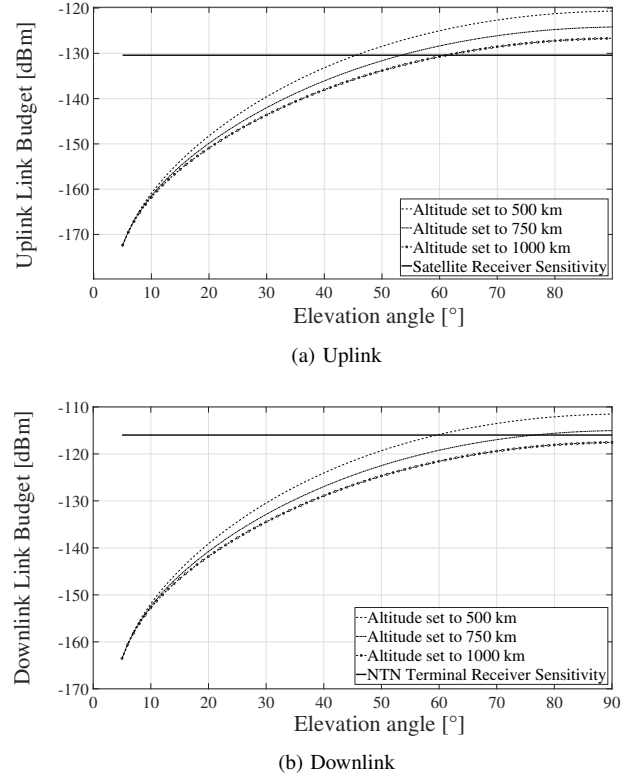


Fig. 3. Link Budget in the function of Elevation Angle for different orbital altitudes.

model real phenomena that impair the signal propagation in both uplink and downlink directions. Therefore, according to the analytical description of the satellite link carried out in [42], the link budget is expressed in dB as a function of both frequency carrier f_c and elevation angle θ_{el} :

$$LB(\theta_{el}, f_c) = P + G_{ANT}(f_c) - FSPL(\theta_{el}, f_c) - L_{imp}(\theta_{el}, f_c) + DCF(\theta_{el}, f_c), \quad (1)$$

where P represents the signal power, G_{ANT} is the sum of the base station and NTN terminal antenna gains (reported in Section V-A), $FSPL$ describes the free space path loss, L_{imp} provides additional losses due to the propagation, and DCF is the sum, expressed in dB, of the diagram correction factors of transmitting and receiving antennas. Note that Eq. (1) does not consider multi-path fading models because the paths due to obstacles on Earth are negligible if compared to the one reaching the satellite. The amount of impairments L_{imp} , instead, is calculated by considering the air attenuation that takes into account the dry air absorption [43], the rainfall attenuation that estimates the droplet absorption, as described in [44], [45], the scintillation attenuation that takes into account the fluctuations of the amplitude and the phase of a radio wave [41], the polarization attenuation that considers the difference between the polarization of both receiving antenna and incoming radio wave [42], and the fog and atmospheric gas absorption [46], [47]. The models used to evaluate the attenuation due to air, rainfall, scintillation and atmospheric gas absorption are predictive models, based on estimates defined analytically in

the most recent updates of the ITU-R recommendations cited above.

Fig. 3 reports the link budget evaluated as a function of the elevation angle and the satellite altitude. Without loss of generality, it is considered an NTN terminal deployed in the European field of view. In line with NB-IoT specifications [21], the carrier frequency and the transmission power have been set to $f_c=1995$ MHz and $P=23$ dBm, respectively, for the uplink. In the downlink, instead, they have been set to $f_c=2185$ MHz and $P=33$ dBm, respectively. Overall, the link budget strongly depends on the user-satellite elevation angle: it increases when the elevation angle progressively approaches 90° . At the same time, the link quality decreases with the satellite altitude. In both uplink and downlink, the receiver antenna captures the attenuated signal and the noise power. Therefore, it is important to understand in which conditions the power of the received signal is higher than the receiver sensitivity. Now, according to [42], the receiver sensitivity represents the noise power of the link expressed by the Nyquist formula reported in Eq. (2):

$$RS|_{dBm} = 30 + 10\log_{10}(k_B T_{sys} BW), \quad (2)$$

where k_B is Boltzmann constant, T_{sys} is the equivalent system noise temperature accounting for both antenna and receiver noise, and BW is the NB-IoT subcarrier bandwidth. According to [48], $T_{sys} = 150$ °K for the uplink and $T_{sys} = 290$ °K for the downlink. On the other hand, instead, BW depends on the chosen transmission configuration.

To conclude, Fig. 3 also reports the calculated receiver sensitivity. Obtained results invite to select the lowest satellite altitude (i.e., 500 km) to reach a suitable link budget for smaller elevation angles. An altitude of 500 km provides the best trade-off between elevation angle (which determines coverage area) and connectivity (expressed in terms of power level perceived by the receiver).

Given the link budget and the receiver sensitivity, it is possible to calculate the expected value of Signal to Noise Ratio (SNR):

$$SNR = LB(\theta_{el}, f_c) - RS. \quad (3)$$

Fig. 4 depicts the SNR curves as a function of the elevation angle for different transmission modes in the uplink. NB-IoT technology allows using subcarriers individually in order to ensure a greater concentration of power on a narrower band. This results in increasing the coverage range and power gain. The marked improvement in the single-tone configuration (almost 10.8 dB if compared to multi-tone) makes this solution more attractive for the conceived architecture. As shown in Fig. 4, the single-tone configuration achieves good SNR values for lower elevation angles with respect to multi-tone. As explained in Section II-A, even if the adoption of a single-tone configuration with a subcarrier of 3.75 kHz would further increase the SNR, this comes at a cost of a longer subframe duration. Therefore, the intermediate configuration (single-tone with a subcarrier of 15 kHz bandwidth) is selected as the best trade-off between SNR performance and time resources

employment. In fact, it guarantees higher SNR with the same elevation angle if compared to multi-tone configuration.

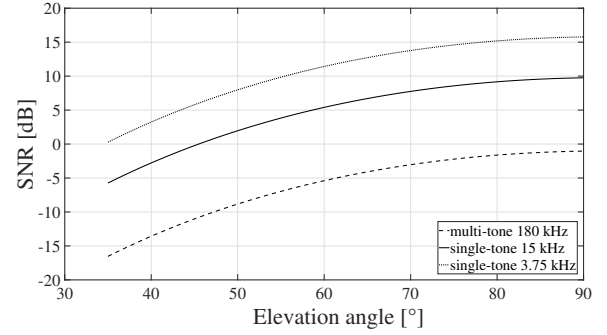


Fig. 4. SNR in different transmission mode configurations for the uplink.

In line with these considerations, BW is set to 15 kHz for the uplink and 180 kHz for the downlink. The receiver sensitivity differs for uplink and downlink configurations. In fact, considering a subcarrier bandwidth of 15 kHz, the uplink communication experiences a lower receiver sensitivity compared to the downlink one, calculated for a subcarrier bandwidth of 180 kHz, resulting in -130 dBm and -117 dBm, respectively.

Note that the intersections between the link budget curves and the receiver sensitivity, shown in Fig. 3, identifies the elevation angle after which the SNR is greater than zero. Nevertheless, the radio link could be established even at negative SNRs under certain configurations, resulting in lower elevation angles. The practical feasibility of the connection is determined by the investigation of the communication success probability defined by the study of the Block Error Rate (BLER) curves, as reported in Section VI-B.

C. Satellite Constellation

The employment of a single satellite per orbit for the chosen 500 km altitude results in very short periods of visibility. On the contrary, considering a constellation of multiple satellites, NTN terminals may have more occasions to transmit their data, thus reducing the periods during which they remain without satellite coverage. This would also lower the amount of data stored and forwarded by each NTN terminal while simplifying the satellite hardware and reducing the NTN terminals energy consumption (which is an important requirement for the IoT technology).

The satellite platform of interest for this study must adopt cheaper solutions, able to satisfy the cost optimization requirement. From this point of view, this work assumes to adopt either small or nano-satellites, providing an effective and low-cost solution with several simplifications in the system design and deployment. Taking this aspect into account, the choice fell on a 12U CubeSat in a 2x2x3 configuration [49]. This platform is composed of several units that can be assembled in a fully scalable and flexible fashion to reach the needed performance.

A LEO Cubesat operating at the altitude of 500 km (corresponding to an orbital radius equal to 6878.14 km) presents a

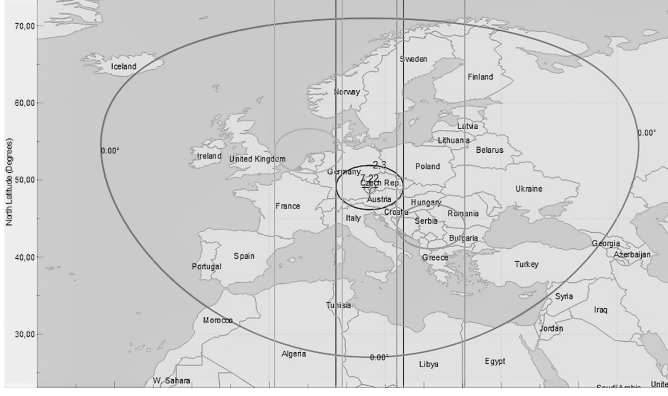


Fig. 5. European field of view and satellite beam coverage.

flying speed needed to maintain the satellite in orbit equal to 7612.6 m/s.

Accordingly, the orbital period is equal to 1 hour and 34 minutes. The number of satellites per orbit must be properly selected to jointly achieve cost and service requirements. A lower number of satellites is surely preferable from the cost perspective. At the same time, however, it is also necessary to consider the low variability of the frequency of sensed data transmission, as well as the battery life of NTN terminals. Thus, to achieve a suitable trade-off between the two aforementioned constraints, the proposed architecture integrates 2 or 3 satellites per orbit. In the first case, an NTN terminal can see a satellite every 47 minutes and 18 seconds, even if the 500 km orbital period for a single satellite is of 1 hour and 34 minutes. In the latter case, instead, an NTN terminal can see a satellite every 31 minutes and 32 seconds.

The well-known System Tool Kit [50] is used to evaluate the satellite spot-beam diameter. Specifically, according to the goal to cover about 6700 km of longitude corresponding to the European field, the performed investigation highlighted that about 8 circular orbits (i.e., with a 0° eccentricity) and sun-synchronous (i.e., with a $97^\circ/98^\circ$ orbital inclination) are required to ensure the continuous service requirement. In this way, the whole satellite constellation should involve 24 satellites.

Fig. 5 reports the covered geographical area and shows a snapshot of beam coverage and satellite orbits. It is important to note that the areas covered by the satellite beams that belong to adjacent orbits present an overlap. Nevertheless, in order to avoid interference among satellite transmissions on NTN terminals, the solution proposed herein assumes that satellites of different orbits are spatially shifted (as depicted in Fig. 5).

VI. SYSTEM-LEVEL PERFORMANCE OF NB-IOT OVER SATELLITE

The isolated knowledge of the link budget is not sufficient to evaluate the feasibility of the resulting satellite architecture. For this reason, this Section proves the effectiveness of the proposed architecture through system-level simulations. In particular, the presented analysis evaluates how physical and system configurations influence (1) the ability of the overall

communication architecture to disseminate data through the service-link and (2) the resulting communication latencies.

A. System-level tool and parameter settings

System-level simulations are conducted through the 5G-air-simulator [51] [52]. It represents a well-known system-level simulator, supporting NB-IoT. Among the implemented functionalities, it is important to remark that the model for the Random Access procedure available in 5G-air-simulator has been already validated from an analytical point of view in [53]. This ensures the trustworthiness of the results discussed below. Furthermore, the tool has been properly enhanced to embrace the implementation of the conceived NTN scenario [54].

Regarding the physical layer, the transmitted power and the configured bandwidth used in this study have been already declared in Section V. Other parameters to be configured include: Modulation and Coding Scheme (MCS), TBS, and Number of Resource Units (NRU). The MCS is set to QPSK, since it guarantees a higher spectral efficiency with respect to BPSK. The TBS represents the amount of data passed through the physical layer which will be mapped into the Narrowband-Physical Uplink Shared Channel (NPUSCH) channel. Its value is set to 328 bits, according to the configuration of the protocol stack discussed in Section IV-A. Given the TBS, a data packet can be transmitted by using different NRUs. In line with [55], NRU can be set to 2, 3, 4, 5, or 6. On the one hand, higher values of NRU correspond to a higher data protection level at the physical layer. From another hand, instead, the higher the NRU, the longer-lasting the physical transmission of a data packet. According to the high distances of the considered satellite scenario and the resulting latencies, the upper bound of the number of HARQ retransmissions has been set to 4.

Regarding the Random Access procedure, the number of the available preambles is set to 48, the periodicity of the RAO is set to 80 ms, and the backoff window is set to 65536 ms.

To evaluate the impact of the traffic load, a different number of clusters of NTN terminals are considered. As already anticipated in Section III, each cluster contains 3000 NTN terminals deployed in a single crop field with an area of 30 hectares. Each NTN terminal generates data every 4 hours. Moreover, every 4 hours, all the available NTN terminals generate their data within a time slot of 1 minute. In this way, it is possible to investigate how the designed approach reacts in critical bursty traffic conditions.

The satellite allocates radio resources to NTN terminals that won the access procedure according to the round-robin scheduler.

Finally, computer simulations are conducted to observe 48 hours of network activity. Such an amount of time embraces a large number of satellite visibility cycles and allows obtaining stable average results.

B. Link-to-system model

A link-to-system model represents the first step towards an accurate system-level study. In fact, it is able to describe the

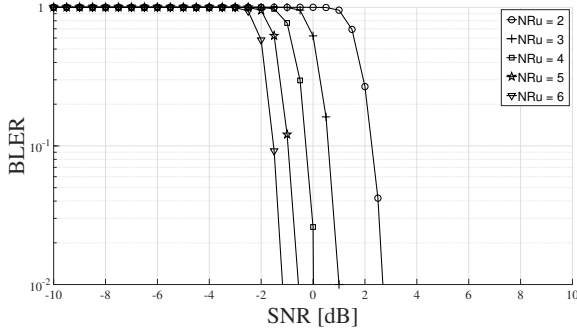


Fig. 6. BLER curves

quality of the communication achieved under specific parameter settings, while ensuring an abstraction of transmission, propagation, and reception aspects. In this context, the 5G-air-simulator tool has been extended to implement the propagation model, link budget, and SNR model, as discussed in Section V. Then, BLER curves have been integrated as well, in order to simulate the quality of the communication link as a function of the measured SNR. To this end, MATLAB LTE Toolbox has been used to generate BLER curves. Given the setting of physical parameters, the BLER has been computed as the ratio between the total number of received blocks for which the control of the Cyclic Redundancy Check (CRC) fails and the total number of transmitted blocks. Furthermore, to achieve a fine-grained BLER evaluation, SNRs values have been chosen in the range spanning from -10 dB to 10 dB. The total number of transmitted blocks has been set to 1000.

Fig. 6 shows the obtained BLER curves as a function of NRU and SNR. Results highlight that higher NRU values provide a better protection of data transmitted at the physical layer. At the same time, higher SNRs values are associated with better link conditions. Thus, based on these premises, it is possible to conclude that the BLER reduces with both NRU and SNR.

C. Satellite attach procedure and visibility time

Each NTN terminal starts the attachment procedure when the receiver power of the reference signal transmitted by the satellite experiences a coupling loss lower than the Maximum Coupling Loss (MCL) threshold, set to 154 dB. Based on the selected parameter settings and the aforementioned MCL threshold, the average SNR value (measured in the downlink direction) is equal to -4.9 dB. Moreover, according to the study reported in Section V-B, this SNR value is obtained for elevation angles equal to 46.3° for the downlink. Such a condition determines the beginning of the visibility time.

Now, considering the satellite altitude of 500 km, a trigonometrical analysis allows calculating the diameter of the effective satellite footprint. Considering the slant range (that is the distance from the NTN terminal and the satellite, calculated as a function of the conceived elevation angle), the diameter of the effective footprint approximately results in 890 km. Indeed, by exploiting the relative speed (i.e., with respect to the Earth) of the LEO satellite equal to 7059 m/s and the aforementioned

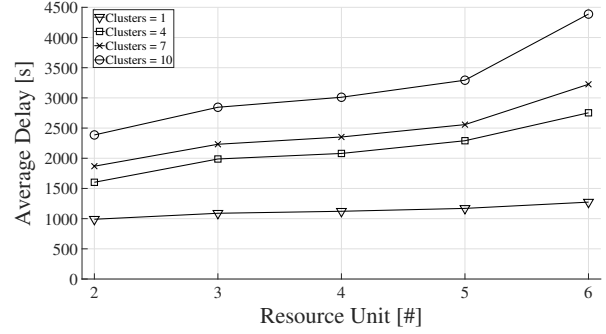


Fig. 7. Average end-to-end delay with EDT disabled.

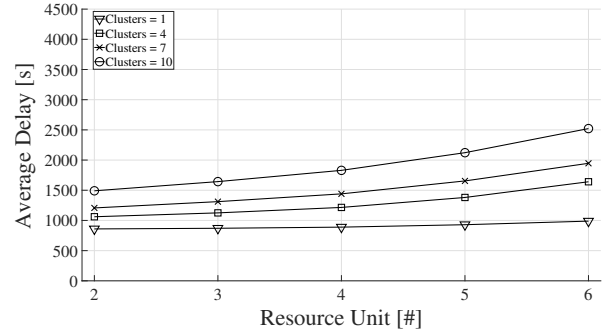


Fig. 8. Average end-to-end delay with EDT enabled.

effective footprint, definitively it is possible to determine the visibility time, approximately equal to 125 s.

D. Communication latencies over the service-link

The communication latency represents the amount of time required by a packet to be successfully received by one of the satellites of the constellation, with respect to its generation time instant. Fig. 7 and Fig. 8 show the communication latency measured when the EDT transmission scheme is disabled and enabled, respectively. Reported curves describe the impact of different physical configurations and different network loads. In this case, each orbit hosts 3 satellites.

First of all, the communication latency depends on the probability to win a Random Access procedure. As expected, a higher number of clusters determines the growth of NTN terminals aiming to access the network and, in turn, the collision probability during the Random Access procedure. This justifies the increment of the communication latency with the number of clusters served by the configured satellite architecture.

Furthermore, also the NRU assigned to each NTN terminal strictly affects the average end-to-end delay. Although a transport block distributed into many Resource Units (RUs) guarantees high protection, it results in a longer transmission time, impacting considerably on end-to-end delay.

On the contrary, the EDT scheme ensures the reduction of the communication latency up to 40%, thanks to its ability to delivery of the data packet along with the Msg3 of the Random Access procedure.

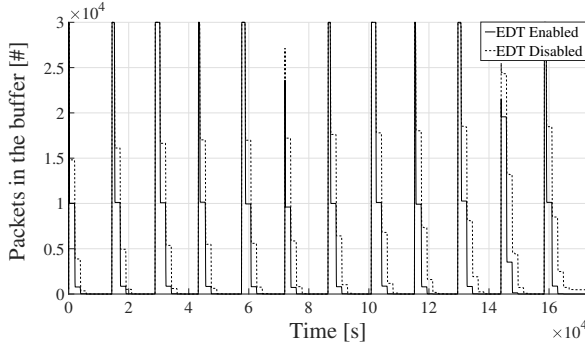


Fig. 9. Number of packets in the buffer with 10 clusters.

TABLE II
AVERAGE COMMUNICATION LATENCY MEASURED UNDER DIFFERENT
CONSTELLATION DESIGNS.

RACH Configuration	Satellites per orbit	Average end-to-end delay [s]			
		$n_C = 1$	$n_C = 4$	$n_C = 7$	$n_C = 10$
EDT disabled	3	969	1602	1869	2386
	2	1816	2739	3124	3895
EDT enabled	3	859	1061	1207	1491
	2	1646	1909	2128	2546

E. Ability of the system to drain buffered data through the service-link

The analysis of the aggregate number of packets stored in all the NTN terminals allows verifying whether the designed satellite architecture is able to successfully support the offered service. If this value quickly grows, it means that the network cannot satisfy all the requests made by the NTN terminals. Consequently, the generated messages will overload the network. On the contrary, if packets in the buffer do not accumulate very fast, the network can absorb the traffic generated by the NTN terminals.

Fig 9 demonstrates the effective ability of the designed approach to drain buffered data through the service-link, considering a constellation of 24 satellites (i.e., 3 satellites per orbit). Without loss of generality, results only refer to the highest loaded scenario (10 clusters of NTN terminals, i.e., 30000 nodes), where NRU is set to 2. Reported curves highlight that NTN terminals need more than one visibility time to transmit their data. The dissemination of the whole packet burst generated by the NTN terminals is faster when EDT is enabled.

F. Impact of the number of satellites per orbit

To provide further insight, Tab. II reports the average communication latency measured when a different number of satellites per orbit is taken into account. As for the previous analysis, the study is conducted by considering NRU equal to 2. As expected, communication latency increases with the number of clusters (n_C). Moreover, EDT always ensures better results. Nevertheless, a constellation with 2 satellites per orbit is still able to drain all the generated data but at the cost of higher communication latency.

VII. CONCLUSION

This work presented an effective NB-IoT over satellite architecture supporting an agriculture use case. In this context, the link-level features were properly investigated through the choice of the suitable antennas and the definition of the proper parameters (satellite altitude, elevation angle, and physical transmission settings) allowing the link reliability. Based on these outcomes, and in line with the recent 3GPP discussions on Non-Terrestrial Networks (NTN) scenarios, the satellite constellation and the resulting architecture were defined. Here, the assumption of the whole protocol stack installed on-board the satellite represents an important novelty that characterizes this work against the current state of the art. Moreover, technical adaptations to the radio interface were explored to fully support the connection between NTN terminals and the remote satellite. Finally, the overall performance was evaluated through system-level simulations, by justifying the design choices taken to satisfy NB-IoT specifications and offer exhaustive proof of the feasibility of the conceived solution. Future research activities will explore other use cases, address any novel required extension, and evaluate the effectiveness of the proposed technical solutions through an experimental testbed. Regarding this latter important aspect, the work will implement terminals and base stations through Software-Defined Radio, NB-IoT traffic emulator, and channel emulator through hardware/software modules. The intention is to meet a Technology Readiness Level higher than 4.

REFERENCES

- [1] K. Mekki, E. Bajic, F. Chaxel, and F. Meyer, "A comparative study of LPWAN technologies for large-scale IoT deployment," *ICT Express*, vol. 5, no. 1, pp. 1 – 7, 2019. [Online]. Available: <http://www.sciencedirect.com/science/article/pii/S2405959517302953>
- [2] O. Kodheli, N. Maturo, S. Andrenacci, S. Chatzinotas, and F. Zimmer, "Link budget analysis for satellite-based narrowband IoT systems," in *International Conference on Ad-Hoc Networks and Wireless*. Springer, 2019, pp. 259–271.
- [3] G. Charbit, D. Lin, K. Medles, L. Li, and I. Fu, "Space-terrestrial radio network integration for IoT," in *2nd 6G Wireless Summit (6G SUMMIT)*, 2020, pp. 1–5.
- [4] K. O'Hara and G. Skidmore, "Providing narrowband IoT coverage with Low Earth Orbit satellites," *Microwave Journal*, vol. 62, no. 12, pp. 74–84, 2019.
- [5] Z. Qu, G. Zhang, H. Cao, and J. Xie, "LEO satellite constellation for Internet of Things," *IEEE Access*, vol. 5, pp. 18 391–18 401, 2017.
- [6] S. Cluzel, L. Franck, J. Radzik, S. Cazalens, M. Dervin, C. Baudoin, and D. Dragomirescu, "3GPP NB-IoT Coverage Extension using LEO Satellites," in *IEEE 87th Vehicular Technology Conference (VTC Spring)*, 2018, pp. 1–5.
- [7] A. K. Dwivedi, S. Praneeth Chokkarapu, S. Chaudhari, and N. Varshney, "Performance analysis of novel Direct Access schemes for LEO satellites based IoT network," in *IEEE 31st Annual International Symposium on Personal, Indoor and Mobile Radio Communications*, 2020, pp. 1–6.
- [8] O. Kodheli, S. Andrenacci, N. Maturo, S. Chatzinotas, and F. Zimmer, "An uplink UE Group-Based Scheduling Technique for 5G mMTC systems over LEO satellite," *IEEE Access*, vol. 7, pp. 67 413–67 427, 2019.
- [9] M. Conti, S. Andrenacci, N. Maturo, S. Chatzinotas, and A. Vanelli-Coralli, "Doppler Impact Analysis for NB-IoT and Satellite Systems Integration," in *IEEE International Conference on Communications (ICC)*, 2020.
- [10] O. Kodheli and N. Maturo and S. Chatzinotas and S. Andrenacci and F. Zimmer, "On the Random Access procedure of NB-IoT Non-Terrestrial Networks," in *10th Advanced Satellite Multimedia Systems Conference (ASMS) and 16th Signal Processing for Space Communications Workshop (SPSC)*, 2020, IEEE Virtual Conference.

- [11] A. Guidotti, A. Vanelli-Coralli, M. Conti, S. Andrenacci, S. Chatzinotas, N. Maturo, B. Evans, A. Awoseyila, A. Ugolini, T. Foggi *et al.*, "Architectures and key technical challenges for 5G systems incorporating satellites," *IEEE Transactions on Vehicular Technology*, vol. 68, no. 3, pp. 2624–2639, 2019.
- [12] 3GPP, "Solutions for NR to support non-terrestrial networks (NTN)," 3rd Generation Partnership Project (3GPP), Technical Report (TR) 38.821, 2018, Release 16.
- [13] —, "[IoT-NTN] Applicability of TR 38.821 (MediaTek)," 3rd Generation Partnership Project (3GPP), Discussion, Decision R2-2011275, November 2020, RAN WG2 112e.
- [14] Y. E. Wang, X. Lin, A. Adhikary, A. Grovlen, Y. Sui, Y. Blankenship, J. Bergman, and H. S. Razaghi, "A primer on 3GPP Narrowband Internet of Things," *IEEE Communications Magazine*, vol. 55, no. 3, pp. 117–123, 2017.
- [15] H. Malik, H. Pervaiz, M. Mahtab Alam, Y. Le Moullec, A. Kuusik, and M. Ali Imran, "Radio resource management scheme in NB-IoT systems," *IEEE Access*, vol. 6, pp. 15 051–15 064, 2018.
- [16] 3GPP, "E-UTRA and E-UTRAN; LTE Physical Layer, General Description," 3rd Generation Partnership Project (3GPP), Technical Specification (TS) 36.201, 2018, Release 15.
- [17] —, "E-UTRA and E-UTRAN; LTE Physical Layer, Overhaul Description," 3rd Generation Partnership Project (3GPP), Technical Specification (TS) 36.300, 2018, Release 15.
- [18] R. Ratasuk, N. Mangalvedhe, Y. Zhang, M. Robert, and J. Koskinen, "Overview of narrowband IoT in LTE Rel-13," in *IEEE Conference on Standards for Communications and Networking (CSCN)*, 2016, pp. 1–7.
- [19] A. Guidotti, A. Vanelli-Coralli, T. Foggi, G. Colavolpe, M. Caus, J. Bas, S. Cioni, and A. Modenini, "LTE-based Satellite Communications in LEO Mega-Constellations," *International Journal of Satellite Communications and Networking*, 2017.
- [20] O. Kodolli, A. Guidotti, and A. Vanelli-Coralli, "Integration of satellites in 5G through LEO constellations," in *IEEE Global Communications Conference (GLOBECOM 2017)*, 2017, pp. 1–6.
- [21] 3GPP, "Study on New Radio (NR) to support non-terrestrial networks (NTNs)," 3rd Generation Partnership Project (3GPP), Technical Specification (TS) 38.811, 2020, Version 15.2.0, Release 15.
- [22] C. B. Mwakwata, H. Malik, M. Mahtab Alam, Y. Le Moullec, S. Parand, and S. Mumtaz, "Narrowband Internet of Things (NB-IoT): From physical (PHY) and media access control (MAC) layers perspectives," *Sensors*, vol. 19, no. 11, p. 2613, 2019.
- [23] T. Ojha, S. Misra, and N. Raghuvanshi, "Wireless sensor networks for agriculture: The state-of-the-art in practice and future challenges," *Comput. Electron. Agric.*, vol. 118, pp. 66–84, 2015.
- [24] K. Goel and A. K. Bindal, "Wireless sensor network in precision agriculture: A survey report," in *2018 Fifth International Conference on Parallel, Distributed and Grid Computing (PDGC)*, 2018, pp. 176–181.
- [25] G. Castellanos, M. Deruyck, L. Martens, and W. Joseph, "System assessment of wusn using nb-iot uav-aided networks in potato crops," *IEEE Access*, vol. 8, pp. 56 823–56 836, 2020.
- [26] "Satellite technologies for IoT applications," <https://iotuk.org.uk/wp-content/uploads/2017/04/Satellite-Applications.pdf>, Accessed: 2019-01-29.
- [27] "Development guide for agriculture using NB-IoT," <https://www.gsma.com/iot/resources/guide2-nbiot-agriculture>, Accessed: 2018-10-05.
- [28] H. Jawad, R. Nordin, S. Gharghan, A. Jawad, and M. Ismail, "Energy-Efficient Wireless Sensor Networks for Precision Agriculture: A Review," *Sensors*, vol. 17, no. 8, 2017. [Online]. Available: <https://www.mdpi.com/1424-8220/17/8/1781>
- [29] D. Brunelli, A. Albanese, D. d'Acunto, and M. Nardello, "Energy neutral machine learning based IoT device for pest detection in precision agriculture," *IEEE Internet of Things Magazine*, vol. 2, no. 4, pp. 10–13, 2019.
- [30] M. M. Islam, M. S. Hossain, R. K. Reza, and A. Nath, "IoT based automated solar irrigation system using mqtt protocol in charandeep chakaria," in *2019 1st International Conference on Advances in Science, Engineering and Robotics Technology (ICASERT)*, 2019, pp. 1–6.
- [31] R. Maheswari, H. Azath, P. Sharmila, and S. Sheeba Rani Gnanamalar, "Smart village: Solar based smart agriculture with IoT enabled for climatic change and fertilization of soil," in *2019 IEEE 5th International Conference on Mechatronics System and Robots (ICMSR)*, 2019, pp. 102–105.
- [32] J. P. Shanmuga Sundaram, W. Du, and Z. Zhao, "A survey on lora networking: Research problems, current solutions, and open issues," *IEEE Communications Surveys Tutorials*, vol. 22, no. 1, pp. 371–388, 2020.
- [33] GSMA, "NB-IoT deployment guide to basic feature set requirements," GSM Association and others, Tech. Rep., 2019. [Online]. Available: <https://www.gsma.com/iot/wp-content/uploads/2019/07/201906-GSMA-NB-IoT-Deployment-Guide-v3.pdf>
- [34] 3GPP, "General Packet Radio Service (GPRS) enhancements for Evolved Universal Terrestrial Radio Access Network (E-UTRAN) access," 3rd Generation Partnership Project (3GPP), Technical Specification (TS) 23.401, 2020, Release 16.
- [35] Z. Shelby, K. Hartke, and C. Bormann, "The Constrained Application Protocol (CoAP)," RFC 7252, Jun. 2014. [Online]. Available: <https://rfc-editor.org/rfc/rfc7252.txt>
- [36] 3GPP, "Evolved Universal Terrestrial Radio Access (E-UTRA); Packet Data Convergence Protocol (PDCP) specification," 3rd Generation Partnership Project (3GPP), Technical Report (TS) 36.323, 2020, Release 16.
- [37] —, "Evolved Universal Terrestrial Radio Access (E-UTRA); Radio Link Control (RLC) protocol specification," 3rd Generation Partnership Project (3GPP), Technical Report (TS) 36.322, 2020, Release 16.
- [38] —, "Evolved Universal Terrestrial Radio Access (E-UTRA) Medium Access Control (MAC) protocol specification," 3rd Generation Partnership Project (3GPP), Technical Report (TS) 36.321, 2020, Release 16.
- [39] —, "LTE; Evolved Universal Terrestrial Radio Access (E-UTRA); Physical layer procedures," 3rd Generation Partnership Project (3GPP), Technical Report (TR) 36.213, 2020, Release 14.
- [40] —, "FL Summary on enhancements on UL time and frequency synchronization for NR NTN," 3rd Generation Partnership Project (3GPP), Discussion, Decision R1-2009748, November 2020, RAN WG1 103e.
- [41] C. A. Balanis, *Antenna Theory: Analysis and Design*, 2nd Edition. Wiley, 1996.
- [42] L. J. Ippolito, *Satellite Communications Systems Engineering: Atmospheric Effects, Satellite Link Design and System Performance*, 2nd Edition. Wiley, 2017.
- [43] ITU, "Attenuation by atmospheric gases and related effects," International Telecommunication Union (ITU), Recommendation, 2019, ITU-R P.676-12.
- [44] —, "Propagation data and prediction methods required for the design of Earth-space telecommunication systems," International Telecommunication Union (ITU), Recommendation, 2017, ITU-R P.618-13.
- [45] —, "Characteristics of precipitation for propagation modelling," International Telecommunication Union (ITU), Recommendation, 2021, ITU-R P.837-7.
- [46] —, "Attenuation due to clouds and fog," International Telecommunication Union (ITU), Recommendation, 2019, ITU-R P.840-8.
- [47] —, "Propagation data and prediction methods required for the design of Earth-space telecommunication systems," International Telecommunication Union, Tech. Rep., 2015, recommendations Radiowave Propag. ITU-R 618-12.
- [48] N. Grody, "Antenna temperature for a scanning microwave radiometer," *IEEE Transactions on Antennas and Propagation*, vol. 23, no. 1, pp. 141–144, 1975.
- [49] "Payload Specification for 3U, 6U, 12U and 27U," <http://www.planetarysystemscorp.com/web/wp-content/uploads/2017/08/2002367E-Payload-Spec-for-3U-6U-12U-27U.pdf>, Accessed: 2020-12-10.
- [50] "Satellite Design and Operations," <https://www.agi.com/missions/satellite-missions-design>, Accessed: 2020-12-10.
- [51] S. Martiradonna, A. Grassi, G. Piro, and G. Boggia, "5g-air-simulator: An open-source tool modeling the 5g air interface," *Computer Networks*, vol. 173, p. 107151, 2020.
- [52] —, "Understanding the 5G-Air-simulator: a tutorial on design criteria, technical components, and reference use cases," *Computer Networks*, vol. 177, p. 107314, 2020.
- [53] S. Martiradonna, G. Piro, and G. Boggia, "On the evaluation of the nb-iot random access procedure in monitoring infrastructures," *Sensors*, vol. 19, no. 14, p. 3237, 2019.
- [54] A. Petrosino, G. Sciddurlo, S. Martiradonna, D. Striccoli, G. Piro, and G. Boggia, "Wip: An open-source tool for evaluating system-level performance of nb-iot non-terrestrial networks," in *22nd IEEE International Symposium on a World of Wireless, Mobile and Multimedia Networks*, 2021.
- [55] ITU, "Topography for Earth-to-space propagation modelling," International Telecommunication Union (ITU), Recommendation, 2019, ITU-R P.1511.